Nuclear factor of activated T cells (NFATc4) is required for BDNF-dependent survival of adult-born neurons and spatial memory formation in the hippocampus

Giorgia Quadrato[a,1], Marco Benevento[a], Stefanie Alber[a,b], Carolin Jacob[a,b], Elisa M. Floriddia[a,b], Tuan Nguyen[a], Mohamed Y. Elnaggar[a], Christine M. Pedroarena[c,d], Jeffrey D. Molkentin[e,f], and Simone Di Giovanni[a,1]

[a]Laboratory for Neuroregeneration and Repair, Center for Neurology, Hertie Institute for Clinical Brain Research, [c]Department of Cognitive Neurology, and [d]Systems Neurophysiology Group, Werner Reichardt Centre for Integrative Neuroscience, University of Tübingen, 72076 Tübingen, Germany; [b]Graduate School for Cellular and Molecular Neuroscience, University of Tübingen, 72070 Tübingen, Germany; [e]Molecular Cardiovascular Biology and [f]Howard Hughes Medical Institute, Cincinnati Children's Hospital Medical Center, Cincinnati, OH 45229

Edited* by Gerald R. Crabtree, Howard Hughes Medical Institute, Stanford, CA, and approved April 16, 2012 (received for review February 6, 2012)

New neurons generated in the adult dentate gyrus are constantly integrated into the hippocampal circuitry and activated during encoding and recall of new memories. Despite identification of extracellular signals that regulate survival and integration of adult-born neurons such as neurotrophins and neurotransmitters, the nature of the intracellular modulators required to transduce those signals remains elusive. Here, we provide evidence of the expression and transcriptional activity of nuclear factor of activated T cell c4 (NFATc4) in hippocampal progenitor cells. We show that NFATc4 calcineurin-dependent activity is required selectively for survival of adult-born neurons in response to BDNF signaling. Indeed, cyclosporin A injection and stereotaxic delivery of the BDNF scavenger TrkB-Fc in the mouse dentate gyrus reduce the survival of hippocampal adult-born neurons in wild-type but not in NFATc4$^{-/-}$ mice and do not affect the net rate of neural precursor proliferation and their fate commitment. Furthermore, associated with the reduced survival of adult-born neurons, the absence of NFATc4 leads to selective defects in LTP and in the encoding of hippocampal-dependent spatial memories. Thus, our data demonstrate that NFATc4 is essential in the regulation of adult hippocampal neurogenesis and identify NFATc4 as a central player of BDNF–driven prosurvival signaling in hippocampal adult-born neurons.

adult neurogenesis | long-term potentiation | transcription | neural stem cells

New adult hippocampal neurons are generated continuously as a result of a finely tuned and dynamic balance among neural stem cell proliferation, survival, differentiation, and migration. Once integrated into the dentate gyrus (DG) and hippocampal circuitry, adult-born neurons are likely selected for encoding new information that contributes to learning and memory (1–4). Several extrinsic regulators such as neurotrophins and neurotransmitters have been identified as pivotal in the regulation of survival and synaptic integration of new neurons in the adult hippocampus (5–10). However, much less is known about transcription factors and intracellular signaling required to integrate and transduce those signals. Among a number of potential intracellular mechanisms, Ca^{2+} mobilization plays a pivotal role during neuronal survival, maturation, and synapse formation.

A wide range of stimuli can increase the release of stored intracellular calcium including the binding of growth factors to their receptors and activation of voltage-dependent ion channels (11). A rise in intracellular calcium turns on the phosphatase calcineurin, which rapidly dephosphorylates the four members of the cytoplasmic nuclear factor of activated T cell (NFAT) family (NFATc1–4), promoting their nuclear translocation and transcriptional activation (12–14). NFAT family members were described first as essential components of T-cells activation and later as important regulators for the initiation and coordination of the immune response, including B cells and natural killer cells (12). Calcineurin inhibition through the drug cyclosporin A (CsA) prevents NFAT nuclear translocation and transcriptional activity. Also, CsA treatment has been shown to reduce the number and the outgrowth of neuroblasts in the subgranular zone (SGZ) of the DG (15). Interestingly, NFATc4 (*i*) is expressed in the adult DG (16), (*ii*) is regulated by L-type calcium channels and GSK-3 signaling in hippocampal neurons (17), and (*iii*) is activated by BDNF and NMDA in primary neurons where it promotes survival, synaptic plasticity, and axonal outgrowth (18). Taken together, these data suggest NFATc4 as a potential candidate for regulating various stages of neural stem cell maturation in the adult hippocampus because of its ability to integrate and transduce several signaling cues from the neurogenic niche. Therefore, we hypothesized that NFATc4 may play a pivotal role in regulating adult hippocampal neurogenesis and thus also hippocampal-dependent learning and memory.

Indeed, we found that calcineurin-dependent NFATc4 activity is essential for BDNF-dependent survival of adult-born neurons in the DG and for the survival of in vitro-differentiated hippocampal progenitor cells. However, it does not play a role in neural progenitor cell proliferation or differentiation. Finally, the reduced survival of adult-born neurons stemming from the absence of NFATc4 is associated with selective defects in the encoding of hippocampal-dependent spatial memories. Our findings demonstrate a role for NFATc4 in the regulation of adult neurogenesis and provide insights into the molecular and transcription-dependent regulation of neural progenitor cells' survival in the adult hippocampus.

Results

NFATc4 Regulates the Number of Immature Neurons via Calcineurin. To investigate a potential role for NFATc4 in adult hippocampal neurogenesis, we first determined whether NFATc4 is required to maintain the net number of adult-born neurons. To this end, we decided to measure the number of neurons expressing doublecortin (DCX), a reliable marker for the identification of hippocampal adult-generated neurons (19), in the hippocampus of WT and NFATc4$^{-/-}$ mice. We quantified the total number of DCX$^+$ cells throughout the entire DG and found a significant reduction in DCX$^+$ cells in NFATc4$^{-/-}$ mice compared with WT mice (mean ± SEM: WT, 6,228 ± 510; NFATc4$^{-/-}$, 3,415 ± 467; $P < 0.05$, Student's *t* test) (Fig. 1 *A* and *C*). Accordingly, in the

Author contributions: G.Q. and S.D.G. designed research; G.Q., M.B., S.A., C.J., E.M.F., T.N., and M.Y.E. performed research; J.D.M. contributed new reagents/analytic tools; G.Q., M.B., and C.M.P. analyzed data; and G.Q. and S.D.G. wrote the paper.

The authors declare no conflict of interest.

*This Direct Submission article had a prearranged editor.

[1]To whom correspondence may be addressed: E-mail: giorgia.quadrato@uni-tuebingen.de or simone.digiovanni@medizin.uni-tuebingen.de.

See Author Summary on page 8810 (volume 109, number 23).

This article contains supporting information online at www.pnas.org/lookup/suppl/doi:10.1073/pnas.1202068109/-/DCSupplemental.

hippocampus of NFATc4$^{-/-}$ mice we also observed a significant reduction in the number of cells positive for polysialylated neural cell adhesion protein (PSA-NCAM), an antigen also present in migrating neuroblasts (Fig. S1 *A* and *B*) (20). This observation is in agreement with the evidence that DCX and PSA-NCAM often are coexpressed in adult-born neurons during neurogenesis in the DG (19). To corroborate these findings, we next decided to measure the number of newly generated neuronal cells in early postmitotic stages. For this purpose we determined by immunohistochemistry the number of cells positive for calretinin (CR), a marker transiently expressed in the postmitotic stages of adult-born neurons' maturation (21). As expected, we found a significant reduction in CR^{+} cells in NFATc4$^{-/-}$ mice compared with WT mice (mean ± SEM: WT mice, 5,340 ± 946; NFATc4$^{-/-}$ mice, 1,333 ± 337; $P < 0.05$, Student's *t* test) (Fig. 1 *B* and C). To investigate the expression of NFATc4 in hippocampal adult-born neurons, we performed double-immunofluorescence experiments using antibodies against NFATc4, DCX, and CR. Indeed, we found a subpopulation of DCX^{+} and CR^{+} cells expressing NFATc4 (Fig. 1 *D* and *E* and Fig. S2 *A* and *B*), supporting a possible cell-autonomous role of NFATc4 in adult-born neurons by acting as an intracellular signal transducer in a restricted time frame of adult-born neurons' maturation. NFATc4 expression also was detected by immunoblotting from the dissected hippocampus, although at a low level compared with its high expression in the developing brain at embryonic day 13 (E13) (Fig. S3), supporting the observation by immunohistochemistry that NFATc4 is expressed clearly only in a subset of hippocampal cells. As expected, no immunosignal for NFATc4 was observed in NFATc4$^{-/-}$ hippocampus (Fig. 1 *D* and *E*). Because NFAT signaling classically is activated by calcineurin-dependent dephosphorylation (12–14), we next determined if calcineurin acts upstream of NFATc4 in controlling the number of adult-born neurons. We evaluated the number of DCX^{+} cells in NFATc4$^{-/-}$ and WT mice following i.p. delivery of CsA, a highly specific inhibitor of calcineurin phosphatase activity. Notably, CsA passed through the blood–brain barrier, as shown by its high expression in the brain (Fig. S4). Importantly, we found a drastic reduction in the number of hippocampal adult-born neurons in CsA-treated WT mice that phenocopies observations in NFATc4$^{-/-}$ mice (mean number ± SEM: WT mice, 6,568 ± 548; WT CsA-treated mice, 3,949 ± 411; $P < 0.01$, Student's *t* test) (Fig. 1*F*). Remarkably, we observed no difference in the number of DCX^{+} cells in NFATc4$^{-/-}$ mice injected with vehicle or CsA, indicating that calcineurin signals specifically through NFATc4 and that the other members of the NFAT family are not involved in the control of the number of adult-born neurons in the DG (mean number ± SEM: NFATc4$^{-/-}$ mice, 3,054 ± 423; NFATc4$^{-/-}$ CsA-treated mice, 2,805 ± 300) (Fig. 1*F*). Finally, the observation that calcineurin inhibition during adulthood mimics the phenotype of NFATc4$^{-/-}$ mice, along with previous findings that these mutants show no major macroscopic or microscopic abnormalities during development and in adulthood (22), rules out the possibility that the changes observed might have developmental origins.

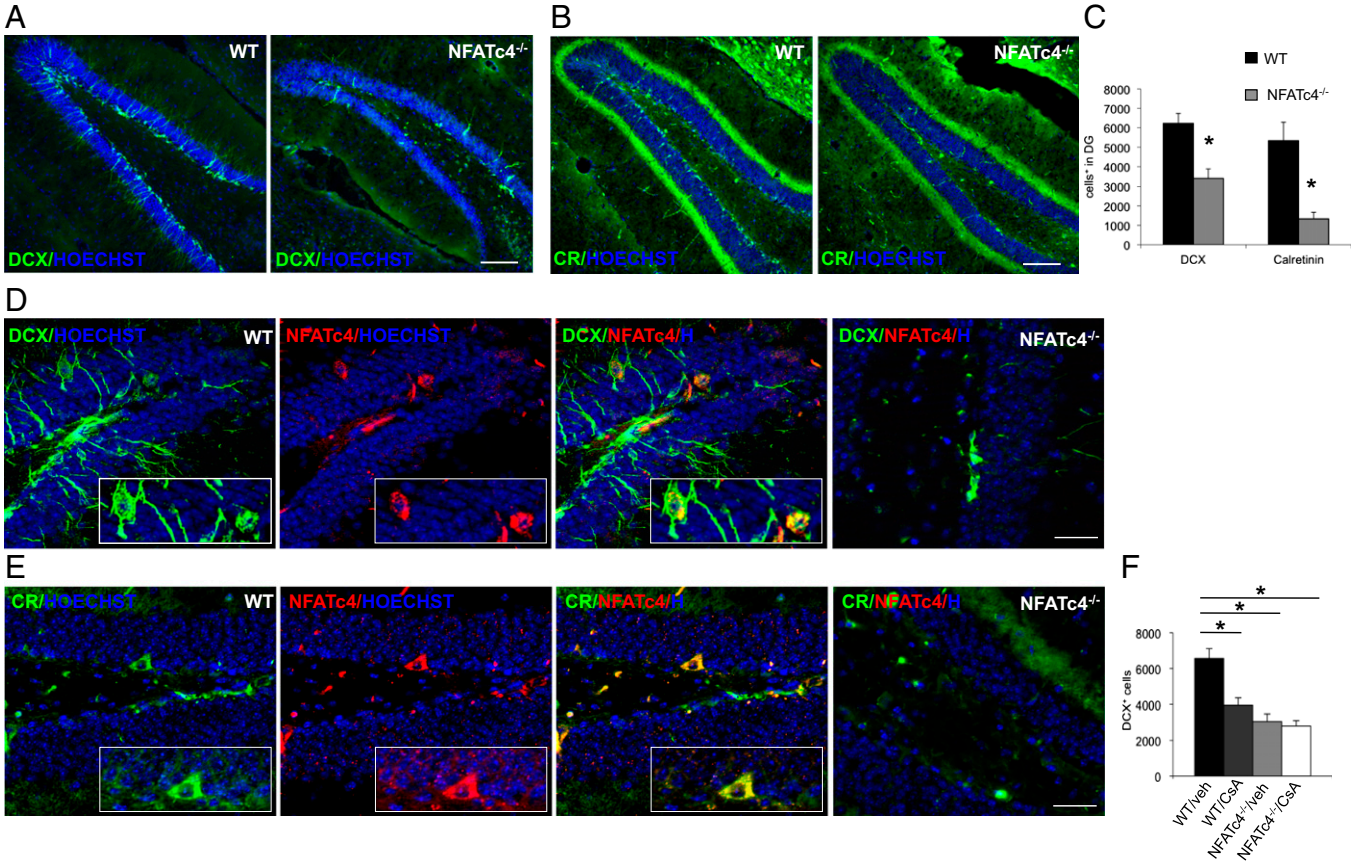

Fig. 1. NFATc4 regulates the number of immature neurons via calcineurin. (*A*) DCX immunostaining (green), and Hoechst labeling (blue) in the DG of WT and NFATc4$^{-/-}$ mice. (*B*) CR immunostaining (green), and Hoechst labeling (blue) in the DG of WT and NFATc4$^{-/-}$ mice. (Scale bars: 100 μm.) (*C*) Quantification of the total number of DCX- and CR-labeled cells in the DG of WT and NFATc4$^{-/-}$ mice. Data represent mean ± SEM, $n = 6$ for DCX; 3 for CR. *$P < 0.05$, Student's *t* test. (*D* and *E*) Immunofluorescence shows NFATc4 (Cell Signaling antibody) (red) colocalization in DCX^{+} cells (green) (*D*) and in CR^{+} cells (green) (*E*). Hoechst labeling is shown in blue. (Scale bars: 40 μm.) (*F*) Quantification of the total number of DCX-labeled cells in the DG of vehicle- and CsA-treated WT and NFATc4$^{-/-}$ mice. Data represent mean ± SEM; $n = 5$ per group. *$P < 0.01$, Student's *t* test.

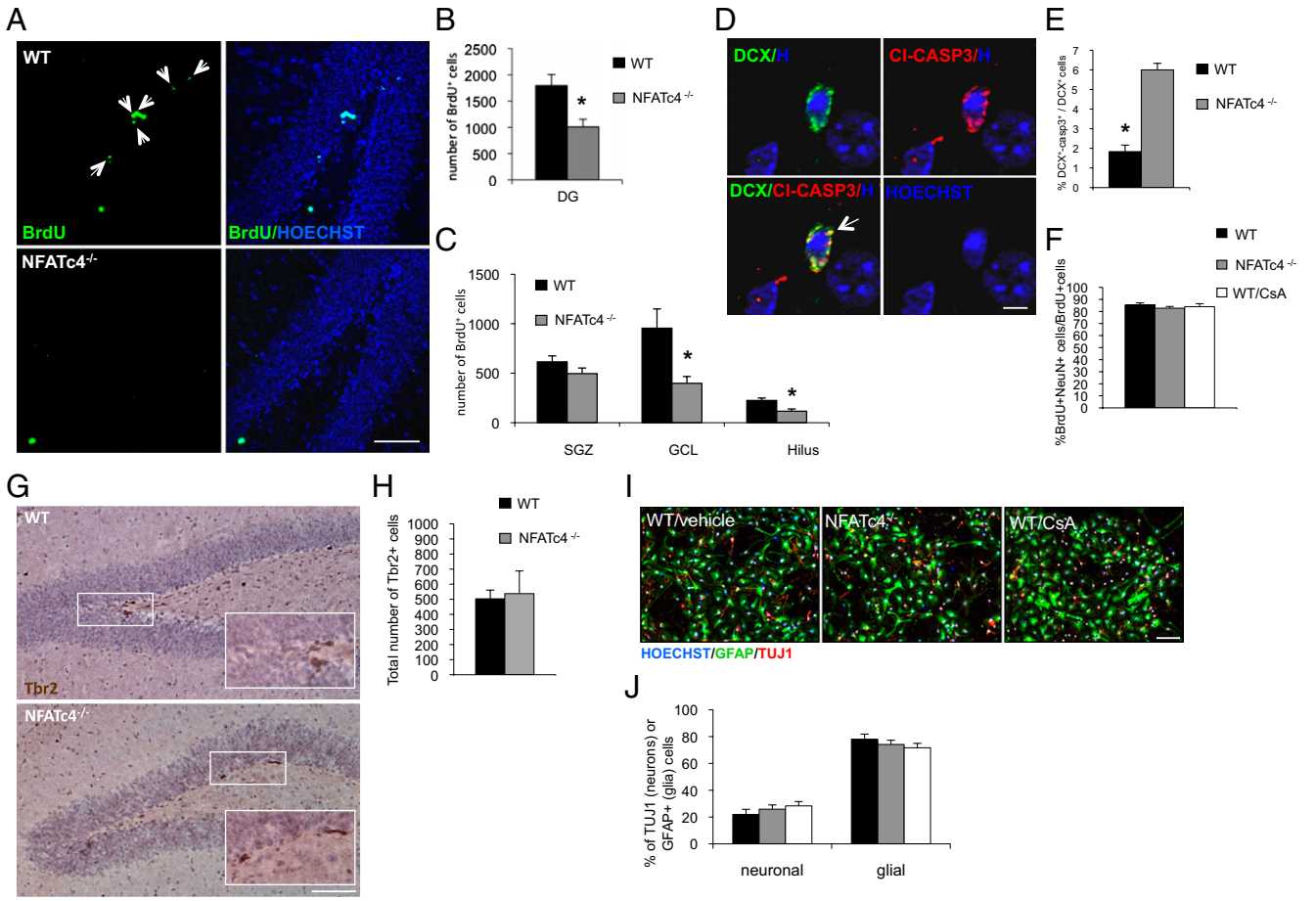

Fig. 2. NFATc4 is required for the survival but not the commitment of adult-born neurons in the DG. (*A*) Immunofluorescence for BrdU (green) and Hoechst staining (blue) in the DG of WT and NFATc4$^{-/-}$ mice. Arrows indicate cells localized in the GCL. (Scale bar: 50 μm.) (*B*) Quantification of BrdU-labeled cells 21 d after BrdU injection in the entire DG of WT and NFATc4$^{-/-}$ mice. Data represent mean ± SEM; $n = 5$ per group. *$P < 0.05$, Student's *t* test. (*C*) Quantification of BrdU-labeled cells in subregions of the DG [SGZ, granular cell layer (GCL), and hilus] of WT and NFATc4$^{-/-}$ mice. Data represent mean ± SEM; $n = 5$ per group. *$P < 0.05$, Student's *t* test). (*D*) Representative picture of an apoptotic DCX$^+$ cell showing DCX (green), cleaved-caspase 3 (red), and Hoechst staining (blue). The arrow indicates a double-labeled cell showing caspase 3 expression and a condensed nucleus next to a healthy-looking nucleus. (Scale bar: 5 μm.) (*E*) Quantification of DCX/cleaved-caspase 3 double-labeled cells expressed as percentage of the total number of DCX$^+$ cells in the entire DG of WT and NFATc4$^{-/-}$ mice. Data represent mean ± SEM; $n = 3$ per group. *$P < 0.05$, Student's *t* test. (*F*) Percentage of BrdU$^+$ cells coexpressing the neuronal lineage marker NeuN$^+$ in the DG of WT, NFATc4$^{-/-}$, and WT CsA-treated mice 21 d after BrdU injection. Data represent mean ± SEM of 80 cells per condition; $n = 3$ per group. (*G*) Tbr2 immunostaining (brown) in the DG of WT and NFATc4$^{-/-}$ mice. (Scale bar: 80 μm.) (*H*) Quantification of the total number of Tbr2$^+$ cells in the entire DG of WT and NFATc4$^{-/-}$ mice. Data represent mean ± SEM; $n = 4$ per group. (*I* and *J*) Percentage of differentiating hippocampal neural progenitor cells versus neuronal (Tuj1$^+$ cells, red) or glial (GFAP$^+$ cells, green) lineages in WT, NFATc4$^{-/-}$, or WT CsA-treated cells (100 ng/mL CsA added in vitro), as determined by immunocytochemistry. Data represent mean ± SEM; $n = 3$; ~100 cells were counted for each condition from at least five randomly chosen fields of view, in three different coverslips. (Scale bar: 100 μm.)

NFATc4 Is Not Required for the Proliferation of Hippocampal Progenitor Cells. In principle, the NFATc4-dependent reduction in the number of adult-born neurons could be caused by an alteration in neural stem cell proliferation, differentiation, impaired cell survival, or by a combination of these events. Importantly, when comparing WT with either NFATc4$^{-/-}$ or CsA-treated mice, we observed no difference in the number of proliferating Ki67-immunopositive cells in the SGZ (mean ± SEM: WT, 3,648 ± 226; NFATc4$^{-/-}$, 3,001 ± 422; WT CsA-treated, 3,200 ± 401) (Fig. S5 *A* and *B*) and in the entire DG (WT, 5,478 ± 294; NFATc4$^{-/-}$, 4,895 ± 343; WT CsA-treated, 5,680 ± 398) (Fig. S5 *A* and *B*). Similarly, and to evaluate directly whether NFATc4 plays a role in precursor cell proliferation, we performed BrdU experiments (150 mg/kg i.p., 2-h pulse) in 3-mo-old NFATc4$^{-/-}$ and WT male mice. As expected, we found that the majority of BrdU$^+$ cells were localized within the SGZ of the adult DG where neural stem cells naturally have access to proliferating signals (Fig. S5*C*). More importantly, we observed no difference in the number of BrdU$^+$ cells between WT and mutant mice in the SGZ (mean ± SEM: WT, 767 ± 87; NFATc4$^{-/-}$, 693 ± 161) (Fig. S5*C*) as well as in the entire DG (mean ± SEM: WT, 1,157 ± 122; NFATc4$^{-/-}$, 1,020 ± 197) (Fig. S5*C*). Accordingly, when hippocampal neurospheres (NSPs) were isolated and cultured in vitro, we did not detect any difference in the proliferation rate by BrdU incorporation regardless of the genotype or treatment with CsA (WT, 10,465 ± 348; NFATc4$^{-/-}$, 10,095 ± 455; WT CsA-treated, 10,561 ± 677) (Fig. S5*D*). Finally, in these cultured cells, no differences were observed in early apoptosis, as detectable with Annexin V positivity, or in late apoptosis, typical of Annexin V propidium iodide double-positive cells (early WT, 4.33 ± 0.29%; late WT, 0.70 ± 0.1%; early NFATc4$^{-/-}$, 3.95 ± 0.17%; late NFATc4$^{-/-}$, 0.7 ± 0.06%) (Fig. S5*E*).

NFATc4 Is Needed for Survival but Not for Fate Commitment of Adult-Born Neurons in the DG. To clarify if the drastic reduction in the number of newborn neurons detected in NFATc4$^{-/-}$ mice is caused by a defect in their survival, we decided to trace and measure the number of surviving BrdU$^+$ cells in WT and NFATc4$^{-/-}$ mice 21 d after BrdU injection. Indeed, the total number of BrdU$^+$ cells in the DG was reduced significantly in

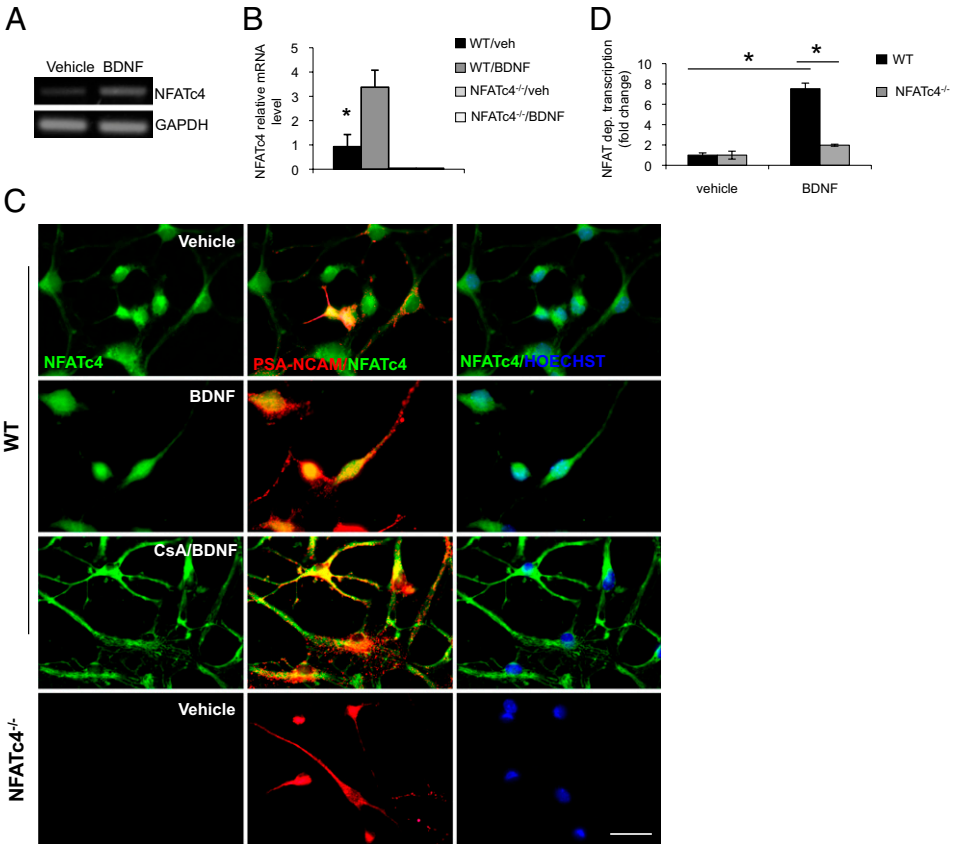

Fig. 3. BDNF promotes NFATc4 expression and activity in vitro. (*A*) RT-PCR analysis for *NFATc4* gene-expression level in hippocampal progenitor cells cultured for 20 h in differentiating conditions in the presence of vehicle or BDNF (100 ng/mL). *GAPDH* was used as a loading control. (*B*) qRT-PCR analysis for NFATc4 gene-expression level in WT and NFATc4$^{-/-}$ cells in the conditions described in *A* normalized to *GAPDH* expression level. Data represent mean ± SEM, $n = 3$. *$P < 0.01$, Student's *t* test. (*C*) Immunofluorescence staining of WT and NFATc4$^{-/-}$ hippocampal progenitor cells cultured for 12 h in differentiating conditions, treated with vehicle, BDNF (100 ng/mL), CsA (100 ng/mL), or BDNF+CsA. NFATc4 (Cell Signaling antibody) (green), PSA-NCAM (red), and Hoechst (blue). (Scale bar: 20 μm.) (*D*) Dual luciferase reporter assay for NFAT transcriptional activity. NFAT relative luciferase activity was calculated as the ratio of Firefly/*Renilla* luciferase signals in WT and NFATc4$^{-/-}$ hippocampal progenitor cells cultured for 12 h in differentiating conditions in the presence of vehicle or BDNF (100 ng/mL). Data represent mean ± SEM; $n = 3$. *$P < 0.01$, Student's *t* test.

NFATc4$^{-/-}$ compared with WT mice (mean ± SEM: WT, 1,795 ± 211.8; NFATc4$^{-/-}$, 1,010 ± 143.6; $P < 0.05$, Student's *t* test) (Fig. 2 *A* and *B*). As expected under these experimental conditions, most of the BrdU^{+} cells in WT mice were localized in the granular cell layer (GCL) of the DG, where the progeny of neural stem cells migrate and differentiate. On the contrary, in NFATc4$^{-/-}$ mice, surviving BrdU^{+} cells were distributed equally between the GCL and the SGZ (Fig. 2*C*) because of a selective reduction in the number of BrdU^{+} cells in the GCL (mean ± SEM: WT, 955 ± 194; NFATc4$^{-/-}$, 398 ± 68.4; $P < 0.05$, Student's *t* test) (Fig. 2*C*) and in the hilus (mean ± SEM: WT, 225 ± 23.9; NFATc4$^{-/-}$, 116 ± 22.7; $P < 0.05$, Student's *t* test) (Fig. 2*C*) but not in the SGZ (mean ± SEM: WT, 615 ± 59.8; NFATc4$^{-/-}$, 496 ± 56.8) (Fig. 2*C*). To verify whether the observed decrease in the survival of progenitor cells also was reflected in a structural difference, we then investigated the overall hippocampal morphology (Fig. S6*A*), the neuronal density (Fig. S6*B*), the volume (Fig. S6*C*), and the total number of granule cells (Fig. S6*D*) of the DG in NFATc4$^{-/-}$ mice and found no differences compared with WT mice. This result might be explained by a possible requirement for NFATc4 in the turnover of hippocampal neurons in the presence of a homeostatic mechanism that keeps the number of granule neurons constant over time. Importantly, in agreement with this view, immunohistochemistry for cleaved-caspase 3 showed a similar number of apoptotic cells in NFATc4$^{-/-}$ and WT mice (Fig. S6*E*). Thus, we hypothesized that NFATc4 might be responsible for the physiological survival and turnover of the select population of adult-born neurons in the DG, which are highly dependent upon the rate of apoptotic cell death. To this end, we performed double immunolabeling for cleaved-caspase 3 and DCX to detect the rate of apoptotic cell death in adult-born neurons of NFATc4$^{-/-}$ and WT mice. As predicted, we found a consistent increase in the number of double-labeled cells in the DG of NFATc4$^{-/-}$ mice (mean ± SEM: WT, 1.83% ± 0.3; NFATc4$^{-/-}$, 6 ± 0.6; $P < 0.05$) (Fig. 2 *D* and *E*), lending support to the idea that NFATc4 is required for the long-term survival of adult-born neurons in the mouse hippocampus. To investigate whether the reduction in the number of adult-born neurons results purely from impairment in cell survival or also from alteration in cell fate commitment, we traced and measured the percentage of BrdU^{+} cells positive for the neuronal marker NeuN 21 d after BrdU injection. We found that the majority of progenitor cells in the DG physiologically commit toward the neuronal lineage in both WT and NFATc4$^{-/-}$ animals as well as in CsA-treated mice (mean ± SEM: WT, 85.4% ± 1.7; NFATc4$^{-/-}$, 82.7% ± 1.43; WT CsA-treated 84 ± 2.5) (Fig. 2*F*). In further support of the evidence that newborn neurons are targeted selectively by NFATc4, we also evaluated the total number of T-box brain gene 2 (Tbr2)-positive cells in the adult DG of WT and NFATc4$^{-/-}$ mice. Tbr2 is expressed in proliferating neuroblasts in a small percentage of DCX- and PSA-NCAM–positive cells but not in CR^{+} cells, suggesting that Tbr2 is down-regulated as progenitors become committed to the neuronal lineage and then exit the cell cycle (23). Importantly, we found no difference in the number of Tbr2^{+} cells in WT and NFATc4$^{-/-}$ mice (mean ± SEM: WT, 503 ± 58; NFATc4$^{-/-}$, 537 ± 150) (Fig. 2 *G* and *H*), further demonstrating that DCX^{+} newborn neurons are targeted selectively in the absence of NFATc4.

In agreement with these in vivo data, neither the absence of NFATc4 nor the inhibition of calcineurin upon CsA treatment influenced neuronal-vs.-glial fate choice in cultured differentiated NSPs (mean ± SEM: WT neuronal, 22 ± 4%; WT glial, 78 ± 4%; WT CsA-treated neuronal, 28 ± 3%; WT CsA-treated glial, 72 ± 3%; NFATc4$^{-/-}$ neuronal, 26 ± 3%; NFATc4$^{-/-}$ glial, 74 ± 3%) (Fig. 2 *I* and *J*), thus ruling out the involvement of NFATc4 activity in the decision-making process for neuronal-vs.-glial differentiation.

NFATc4 Is Expressed in Differentiating Hippocampal Neuroblasts and Promotes Their Survival via BDNF/Calcineurin Signaling. To investigate whether NFATc4 plays a cell-autonomous role in the

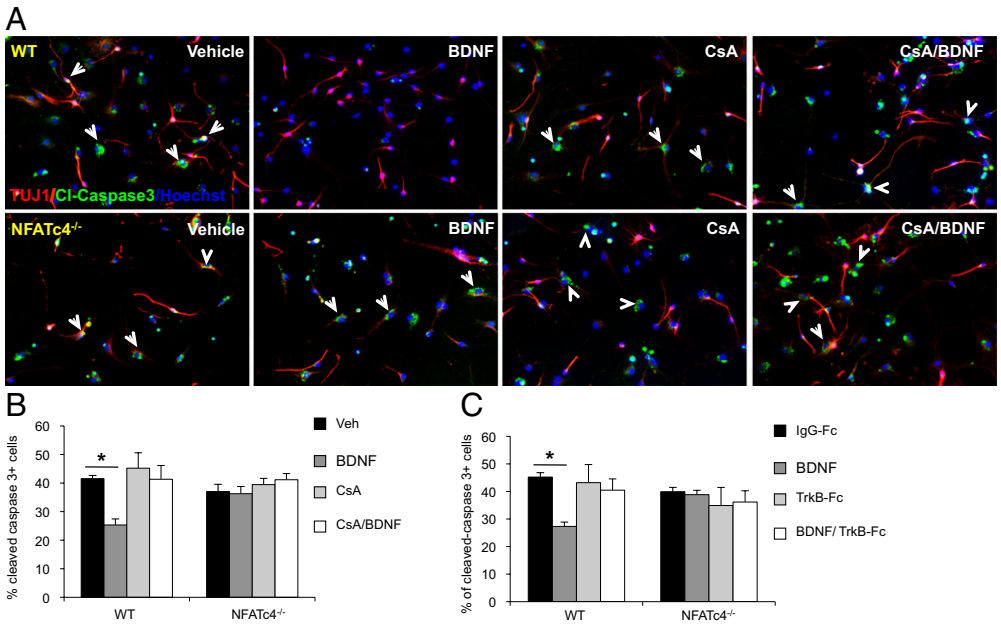

Fig. 4. BDNF is necessary to rescue hippocampal neural progenitor cells from physiological apoptotic death through calcineurin–NFATc4 signaling. (*A*) Immunofluorescence staining (green, cleaved caspase; red, Tuj1; blue, Hoechst) of WT and NFATc4$^{-/-}$ hippocampal progenitor cells cultured for 5 d in differentiating conditions, treated with vehicle, BDNF (100 ng/mL), CsA (100 ng/mL), or BDNF+CsA. Arrowheads show triple-labeled cells. (*B*) Quantification of cleaved-caspase 3–labeled cells, expressed as percentage of the total number of cells (Hoechst staining) in WT and NFATc4$^{-/-}$ hippocampal NSP cultures. Approximately 100 cells were counted in each of at least five randomly chosen fields of view in three different coverslips. Data represent mean ± SEM; $n = 3$. *$P < 0.05$, Student's t test. (*C*) Quantification of cleaved-caspase 3–labeled cells, expressed as percentage of the total number of Hoechst-positive cells in WT and NFATc4$^{-/-}$ hippocampal progenitor cells cultured for 5 d in differentiating conditions, treated with vehicle, IgG1-Fc (333.3 ng/mL), BDNF (100 ng/mL), TrkB-Fc (1 μg/mL), or BDNF+TrkB-Fc. Approximately 100 cells were counted in each of at least five randomly chosen fields of view in three different coverslips. Data represent mean ± SEM; $n = 3$; *$P < 0.05$; t test.

survival of hippocampal differentiating neuroblasts, we performed experiments in cultured adult hippocampal NSPs. First, we found that *NFATc4* indeed was expressed in differentiating NSPs (1 d in vitro) and that administration of 100 ng/mL BDNF, a well-described activator of NFATc4 signaling (24, 25), further enhanced *NFATc4* gene expression significantly (mean ± SEM: vehicle-treated, 1 ± 0.1; BDNF-treated, 3.6 ± 0.2; $P < 0.01$) (Fig. 3 *A* and *B*), but, as expected, no signal for *NFATc4* was detected by real-time RT-PCR in NFATc4$^{-/-}$ cells. Consistent with these data, as shown by immunofluorescence, BDNF also increased NFATc4 expression as well as nuclear localization, whereas CsA blocked these BDNF-dependent events (Fig. 3*C*). Interestingly, the gene expression of another NFAT family member, NFATc2, was not affected by either BDNF or NFATc4 genotype, whereas NFATc3 expression was increased in NFATc4$^{-/-}$ cells and enhanced by BDNF (Fig. S7 *A–C*). As expected, the NFATc4 immunosignal was absent in NFATc4$^{-/-}$ cells but was clearly present in NFATc4$^{-/-}$ NSPs overexpressing NFATc4-EGFP (Fig. S7*D*). Importantly, TrkB, the major receptor for BDNF, also was expressed in these differentiating hippocampal NSPs, as shown by immunofluorescence (Fig. S7*E*). To demonstrate further that BDNF activates NFAT-dependent transcriptional activity, hippocampal NSPs were cotransfected with an artificial luciferase-based reporter construct containing ~500 bp of 1,4,5,-inositol trisphosphate receptor 1, which includes NFAT-specific responsive elements, and with a constitutive active reporter construct. Importantly, under these conditions, BDNF administration significantly increased NFAT-dependent luciferase expression compared with vehicle treatment (mean ± SEM: vehicle, 1 ± 0.2; BDNF, 7.5 ± 0.6; $P < 0.01$) (Fig. 3*D*), supporting the concept that BDNF activates NFATc4-dependent transcription in NSPs. BDNF triggered NFAT-dependent luciferase activity only very modestly and not significantly in NFATc4$^{-/-}$ cells, probably accounting for minor NFATc3-dependent effects, further suggesting NFATc4 as a major player in BDNF signaling in NSPs.

Because BDNF plays an important role in the survival of neuroblasts (5–8), we hypothesized that the prosurvival effects of NFATc4 in adult-born neurons could depend upon BDNF. To verify our hypothesis, we first measured apoptotic cell death during in vitro differentiation of NFATc4$^{-/-}$ and WT adult hippocampal NSPs in the presence of BDNF. Indeed, BDNF rescued the physiological apoptotic death rate, as shown by cleaved-caspase 3 staining in WT cells, but failed to do so in NFATc4$^{-/-}$ cells (mean ± SEM: WT vehicle-treated, 41 ± 1.1%; WT BDNF-treated, 25 ± 2.1%; NFATc4$^{-/-}$ vehicle-treated, 37 ± 2.5%; NFATc4$^{-/-}$ BDNF-treated, 36 ± 2.5%; $P < 0.05$) (Fig. 4 *A* and *B*). In addition, when we codelivered CsA with BDNF, BDNF no longer could rescue apoptotic cell death (mean ± SEM: WT CsA-treated, 45 ± 5.39%; WT CsA/BDNF-treated, 41.3 ± 4.8%; NFATc4$^{-/-}$ CsA-treated, 39.5 ± 2.1%; NFATc4$^{-/-}$ CsA/BDNF-treated, 41.2 ± 2.2%) (Fig. 4 *A* and *B*), supporting the existence of a prosurvival BDNF–calcineurin–NFATc4 axis in hippocampal NSPs. Furthermore, we treated differentiating NSPs with BDNF, TrkB-Fc (a BDNF scavenger) (26), or both. The combination of BDNF and TrkB-Fc selectively blocked the BDNF-dependent rescue of apoptotic cell death in WT cells (mean ± SEM: WT IgG-treated, 45.2 ± 5.5%; WT BDNF-treated, 27.3 ± 1.6%; WT TrkB-Fc–treated: 43.2 ± 6.6%; WT TrkB-Fc/BDNF-treated, 40.46 ± 4.1%; $P < 0.05$) (Fig. 4*C*) but not in NFATc4$^{-/-}$ cells (mean ± SEM: NFATc4$^{-/-}$ IgG-treated, 39.9 ± 3.9%; NFATc4$^{-/-}$ BDNF-treated, 38.8 ± 6.4%; NFATc4$^{-/-}$ TrkB-Fc–treated, 34.9 ± 1.64%; NFATc4$^{-/-}$ TrkB-Fc/BDNF-treated, 36.2 ± 5.4%) (Fig. 4*C*). Finally, to ascertain whether the BDNF–NFATc4 pathway is directly responsible for the survival of differentiating hippocampal NSPs, we overexpressed NFATc4-EGFP or GFP by electroporation and then treated these cells with vehicle or BDNF. In these conditions, we observed a significant rescue of the physiological apoptotic death rate upon codelivery of NFATc4 and BDNF as shown by cleaved-caspase 3 staining (mean ± SEM: GFP/BDNF, 42.5 ± 2.3%; NFATc4/BDNF, 28 ± 3.2%; GFP/vehicle, 40.7 ± 2.6%; NFATc4/vehicle, 37.5 ± 0.7%; $P < 0.05$, Student's t test) (Fig. 5 *A–C*). Taken together these data support the existence of a prosurvival BDNF–calcineurin–NFATc4 axis and suggest that BDNF mediates the survival of cultured hippocampal NSPs by stimulating calcineurin/NFAT activity. Importantly, the total expression levels of *BDNF* (Fig. S8*A*) and of TrkB (Fig. S8 *B* and *C*) did not differ in WT and NFATc4$^{-/-}$ adult hippocampus, suggesting that NFATc4 does not regulate their basal levels but specifically acts downstream of BDNF/TrkB signaling.

A remaining relevant question was whether NFATc4 would play a prominent role in the survival of adult-born neurons

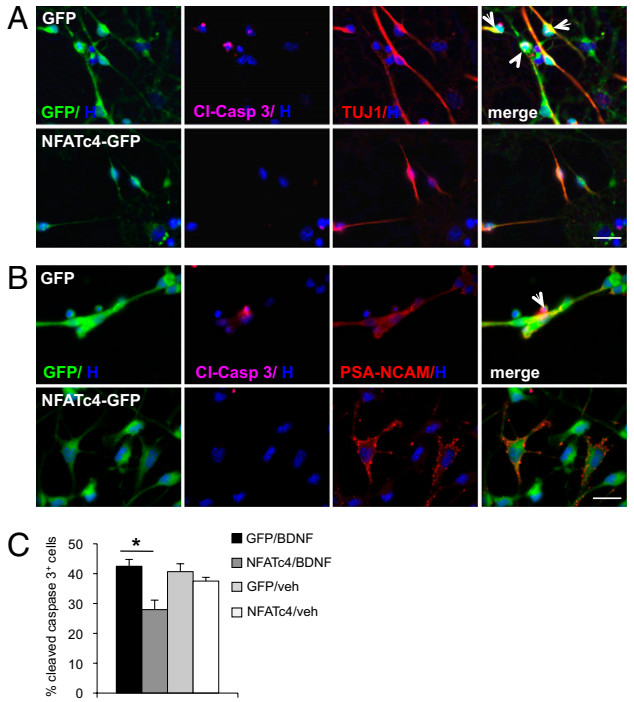

Fig. 5. NFATc4 overexpression rescues differentiating progenitor cells from apoptosis after BDNF administration. (*A*) Split images of vehicle- and BDNF-treated progenitor cells transfected with NFATc4-EGFP or GFP (green) and labeled with Tuj1 (red), cleaved-caspase 3 (pink), and Hoechst (blue). Arrowheads indicate triple-labeled cells. (Scale bar: 20 μm.) (*B*) Split images of vehicle- and BDNF-treated cells transfected with NFATc4-EGFP or GFP (green) and labeled with PSA-NCAM (red), cleaved-caspase 3 (pink), and Hoechst (blue). Arrowhead indicates triple-labeled cell. (Scale bar: 20 μm.) (*C*) Rescue experiment in NFATc4$^{-/-}$ hippocampal progenitor cells transfected with NFATc4-EGFP or GFP plasmids as shown in A and *B*. Data show the rate of apoptosis in transfected cells treated with vehicle or BDNF (100 ng/mL) with 5 d of differentiation. Approximately 100 cells were counted for each of three different coverslips. Data represent mean ± SEM; $n = 3$. *$P < 0.05$, Student's t test.

mediated by BDNF signaling in vivo. To this end, we examined whether the inhibition of BDNF signaling in the adult DG could impair the survival of adult-born neurons in WT but not in NFATc4$^{-/-}$ mice and potentially mimic the NFATc4$^{-/-}$ phenotype. We delivered the BDNF scavenger TrkB-Fc (100 μg, 0.5 μL/h) or its control peptide IgG-Fc, (33.3 μg, 0.5 μL/h) stereotaxically in the DG for 15 d via osmotic minipumps in both WT and NFATc4$^{-/-}$ mice and measured the number of DCX^{+} cells. Although it must be remembered that TrkB-Fc also may inhibit NT4, because of the very low expression of NT4 in the hippocampus as compared with BDNF, it is conceivable that TrkB-Fc might mainly block BDNF signaling. Strikingly, the number of DCX^{+} cells in WT mice treated with TrkB-Fc was significantly reduced, phenocopying the NFATc4$^{-/-}$ genotype (mean ± SEM: WT IgG-treated, 100 ± 27.8%; WT TrkB-Fc–treated, 40.4 ± 8.1%; $P < 0.05$) (Fig. 6 *A* and *B*), but the treatment did not have any effect on the total number of DCX^{+} cells in NFATc4$^{-/-}$ mice (mean ± SEM: NFATc4$^{-/-}$ IgG-treated, 33 ± 9%; NFATc4$^{-/-}$ TrkB-Fc–treated, 30.2 ± 7.9%) (Fig. 6 *A* and *B*). Importantly, the number of hippocampal Ki67^{+} proliferating cells was not affected by the BDNF scavenger in either WT or NFATc4$^{-/-}$ mice (mean ± SEM: WT IgG-treated, 100 ± 10.7%; WT TrkB-Fc–treated, 99.8 ± 8%; NFATc4$^{-/-}$ IgG-treated, 100.3 ± 5.4%; NFATc4$^{-/-}$ TrkB-Fc–treated, 88.9 ± 12.6%) (Fig. 6*C*). In addition, to rule out the possibility that the observed reduction in DCX^{+} cells was caused by an alteration in neuronal fate commitment, we performed double-immunolabeling experiments for BrdU and NeuN in the DG of TrkB-Fc–treated or control mice. Indeed, 2 wk after BrdU injection, we found no significant differences in the percentage of BrdU^{+} cells coexpressing the neuronal lineage marker NeuN, in the four conditions studied (mean ± SEM: WT IgG-treated, 76.7 ± 3.3%; WT TrkB-Fc–treated, 78 ± 3.6%; NFATc4$^{-/-}$ IgG-treated, 81.4 ± 4.7%; NFATc4$^{-/-}$ TrkB-Fc–treated, 79.2 ± 2.1%) (Fig. 6*D*).

NFATc4$^{-/-}$ Mice Show Selective Impairment in the Formation of Spatial Long-Term Memory and Long-Term Potentiation. Several previous studies have indicated a correlation between the number of hippocampal adult-generated neurons and learning and memory (27). Therefore, we decided to assess the performance of NFATc4$^{-/-}$ mice in behavioral tasks that test the formation of hippocampal-dependent memory. First, NFATc4$^{-/-}$ and WT mice were subjected to a fear-conditioning paradigm that evaluates hippocampal-dependent (contextual test) and amygdala-dependent (cued test) long-term reference memory (28–30). During the training session, animals learned to associate a particular cage (context/conditioned stimulus) with a mild foot-shock (aversive stimulus/unconditioned stimulus). Additionally, the foot shock was paired with a tone (cue). After 24 h the animals were put back in the same cage, and the amount of time in which they exhibited a fear response (freezing/conditioned response) (31) was recorded to evaluate the memory of contextual fear conditioning. Also, 48 h after training, mice were tested for auditory-cued fear conditioning in a novel chamber. NFATc4$^{-/-}$ and control WT mice displayed similar levels of freezing to the context (mean ± SEM: WT, 81.9 ± 16.2 s; NFATc4$^{-/-}$, 97 ± 15.6 s) (Fig. 7*A*) and to the tone (mean ± SEM: WT, 16.9 ± 8.5 s; NFATc4$^{-/-}$, 21.2 ± 8s) (Fig. 7*A*), indicating that NFATc4$^{-/-}$ mice are not impaired in either contextual or cued long-term memory.

Next, mice underwent a reference memory version of the Morris water maze, which is among the most frequently used experimental paradigms for the functional assessment of adult neurogenesis (32). NFATc4$^{-/-}$ and control WT mice were analyzed with the standard hidden-platform version of the Morris water maze task (33) and trained with six trials per day for 4 d consecutively. In these conditions, both WT and NFATc4$^{-/-}$ mice were able to learn to navigate to the hidden platform during the 4-d training [as evidenced by a nonsignificant interaction in the mixed model repeated-measures two-way ANOVA; $F_{(3,72)} = 1.67$, genotype × training days]. Interestingly, mutant mice took longer to locate the goal during the last day of training (mean ± SEM; WT day 1, 53.45 ± 4.3 s; WT day 2, 24.1 ± 4.4 s; WT day 3, 24.1 ± 3.2 s; WT d 4, 18.6 ± 2.6 s; NFATc4$^{-/-}$ day 1, 49.2 ± 5 s; NFATc4$^{-/-}$ day 2, 30.9 ± 5 s; NFATc4$^{-/-}$ day 3, 30.2 ± 5.7 s; NFATc4$^{-/-}$ day 4, 34 ± 7.2 s; $P < 0.05$ at day 4 between WT and NFATc4$^{-/-}$ mice; Student's t test) (Fig. 7*B*). Importantly, visual acuity (measured in a cued version of this task), swim speed, and thigmotaxic behavior did not differ between the two groups throughout the training session (Fig. S9 *A–C*).

As expected, when tested in the probe trial conducted on day 5, WT mice spent significantly more time in the target quadrant (NE) than in the other three quadrants (NW, SE, and SW) [mean ± SEM for WT: NE, 39.5 ± 2.6 s; NW, 28.2 ± 2.12 s; SE, 30.0 ± 2.1 s; SW, 22.1 ± 1.7 s; one-way ANOVA; $F_{(3,51)} = 11.19$; $P < 0.0001$; Bonferroni´s multiple comparison test: NE vs. SE, $P < 0.05$; NE vs. SW, $P < 0.01$; NE vs. NW, $P < 0.01$] (Fig. 7*C*). On the contrary, in line with the increased latency time displayed on day 4 of the acquisition phase, NFATc4$^{-/-}$ mice did not show preference for any of the quadrants in the probe trial (Fig. 7*C*) [mean ± SEM NFATc4$^{-/-}$: NE, 31.4 ± 2.6 s; NW, 33.1± 1.9 s; SE, 25.6 ± 1.9 s; SW, 29.7 ± 2.4 s; one-way ANOVA; $F_{(3,51)} = 2.17$], indicating that NFATc4 is required for spatial memory consolidation.

Finally, to exclude the possibility that any perceived memory deficits in NFATc4$^{-/-}$ mice could be caused by physical disability or anxiety, a number of control experiments were performed. We first used the elevated plus maze, a well-established paradigm used to study the anxiety-like behavior (34). The number of entries and the percentage of time spent in the closed and open

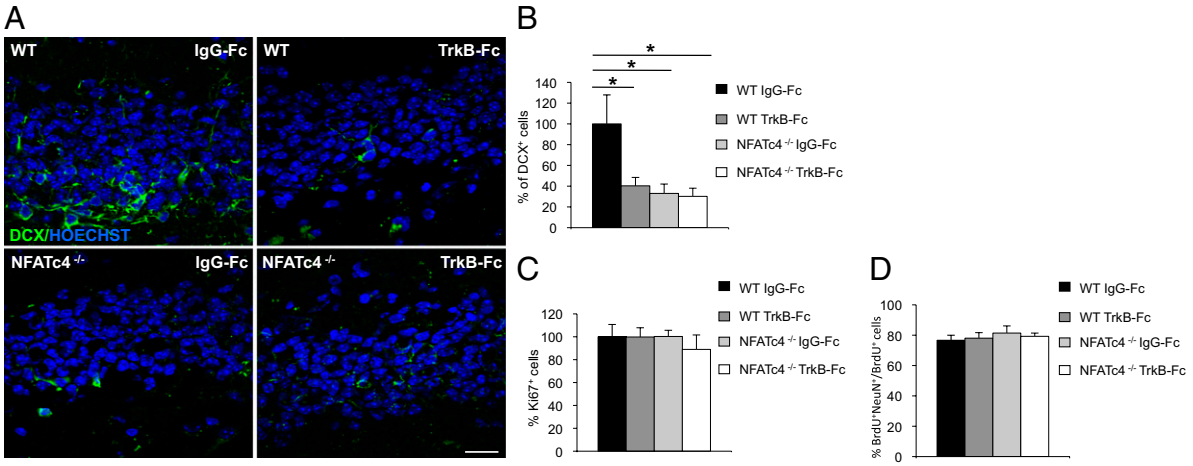

Fig. 6. Inhibition of BDNF signaling decreases the number of hippocampal adult-born neurons in WT but not in NFATc4$^{-/-}$ mice. Both WT and NFATc4$^{-/-}$ mice were infused with IgG1-Fc (33.3 μg, 0.5 μL/h) or TrkB-Fc (100 μg, 0.5 μL/h) over a time period of 15 d via an osmotic minipump into the right hemisphere of the DG. (*A*) Immunofluorescence of DCX (green) and Hoechst (blue) in the DG of WT and NFATc4$^{-/-}$ mice. (Scale bar: 20 μm.) (*B*) Quantification of DCX-labeled cells in the DG of WT and NFATc4$^{-/-}$ mice. Data represent mean ± SEM; $n = 6$ per group. (*C*) Quantification of Ki67-labeled cells in the DG of WT and NFATc4$^{-/-}$ mice. (Data represent mean ± SEM; $n = 3$ per group.) (*D*) Percentage of BrdU$^+$ cells coexpressing the neuronal lineage marker NeuN in the DG of WT and NFATc4$^{-/-}$ mice 15 d after BrdU injection. Data represent mean ± SEM of 80 cells per condition; $n = 3$ per group. *$P < 0.05$, Student's *t* test.

arms and in the center of the maze did not differ between the two genotypes (Fig. S9 *D* and *E*), demonstrating that NFATc4 does not play a role in anxiety-like behavior. Potential differences in pain sensitivity or in locomotion, which may affect the aforementioned tests, were assessed using the plantar heat (Fig. S9*F*) and the automated catwalk paradigms (Fig. S9 *G–I*). Importantly, these experiments showed no significant differences between genotypes, further supporting the specific involvement of NFATc4 in the formation of long-term spatial memory.

Changes in learning and memory could result from changes in synaptic plasticity. To determine whether the absence of NFATc4 leads to changes in synaptic plasticity in the DG, long-term potentiation (LTP) of field postsynaptic potentials (fEPSPS) evoked by activation of the medial perforant path (MPP) was investigated in hippocampal slices obtained from 2- to 4-mo-old WT and NFATc4$^{-/-}$ mice. LTP could be induced effectively by high-frequency trains (100 Hz) in WT but not in NFATc4$^{-/-}$ mice (Fig. 7*D*, *Upper Left*). However, LTP could be induced in NFATc4$^{-/-}$ mice when $GABA_A$-dependent inhibition was blocked (Fig. 7*D*, *Lower Left*). These data indicate that absence of NFATc4 affects the threshold for plasticity induction in the DG when inhibition is intact. They also are in agreement with previous studies showing that a reduction in the number of DG adult-born neurons (35–38), which have a lower threshold for LTP induction than mature ones (39), results in similar impaired LTP formation.

Discussion

NFAT proteins are considered ubiquitous regulators of development, differentiation, and adaptation processes in a wide range of mammalian cells types (40). As activity-dependent transcription factors, they have been shown to be important for the ability of a new tissue to modify the gene-expression profile in response to environmental changes (41). Thus, they also appear ideally suited to regulate the maintenance and adaptation processes that adult-born neurons undergo in neurogenic niches.

Here we demonstrate with several lines of evidence that NFATc4 is selectively required for the survival of hippocampal progenitor cells, because our data both in vitro and in vivo show that NFATc4 does not affect the net rate of neural precursor proliferation or their fate commitment. In addition, we show that calcineurin-dependent activity of NFATc4 is required to mediate BDNF prosurvival signaling in hippocampal adult-born neurons. In fact, the BDNF-dependent increase in survival is fully blocked after inhibition of calcineurin activity.

Our observations are in agreement with the findings that a functional BDNF/TrkB signaling pathway is critical for the survival of adult-born neurons (5–8) but to some extent appears to be dispensable for their proliferation and their fate commitment (7, 42). In the adult DG, newborn neurons are recruited into a functional memory network (49) and exhibit special synaptic plasticity properties, such as a lower threshold in the induction of long-term potentiation (39). Indeed survival of newborn neurons is dependent upon their input synaptic activity (10); interestingly, newborn neurons lacking the full-length TrkB receptor show impaired synaptic plasticity and therefore an increased death rate at the transition from the immature to the mature stage (8). In the CNS, the amount of BDNF is regulated by neuronal activity and is important for the positive selection and survival of functionally active neurons (43). As discussed by Sairanen et al. (7), in the adult DG BDNF may enhance the turnover of dentate granule neurons rather than increasing their total number by enhancing the survival of those neurons that best mediate useful neuronal activity. In this perspective, the young neurons might have a competitive advantage over the older ones because they exhibit special properties in synaptic plasticity that may improve the ability of the hippocampus to adjust rapidly to environmental changes and challenges. A similar model describing the homeostatic plasticity dependent on adult neurogenesis as a key to cell death/survival is discussed by Butz et al. (44) and is consistent with our observation that, despite a consistent increase in the number of apoptotic DCX$^+$ cells in the DG of NFATc4$^{-/-}$ mice, the overall level of apoptosis and the neuronal density of the dentate granule neurons are not affected in NFATc4$^{-/-}$ mice. Based upon these data we propose a model in which NFATc4 acts as an intracellular signal transducer only in a restricted time frame of adult-born neurons' maturation. In particular, it appears to play a role in the late DCX-dependent phase of expression, the stage at the transition between the immature and the mature state, most likely regulating the turnover of hippocampal neurons in the adult DG in response to BDNF signaling. In principle, the impairment in adult hippocampal neurogenesis in NFATc4 mutant mice could result from the absence of NFATc4 in the neural progenitor cells, in their environment, or both. Our in vitro data strongly support a cell-autonomous requirement for calcineurin/NFATc4 signaling in the survival of hippocampal neuronal progenitor cells; however,

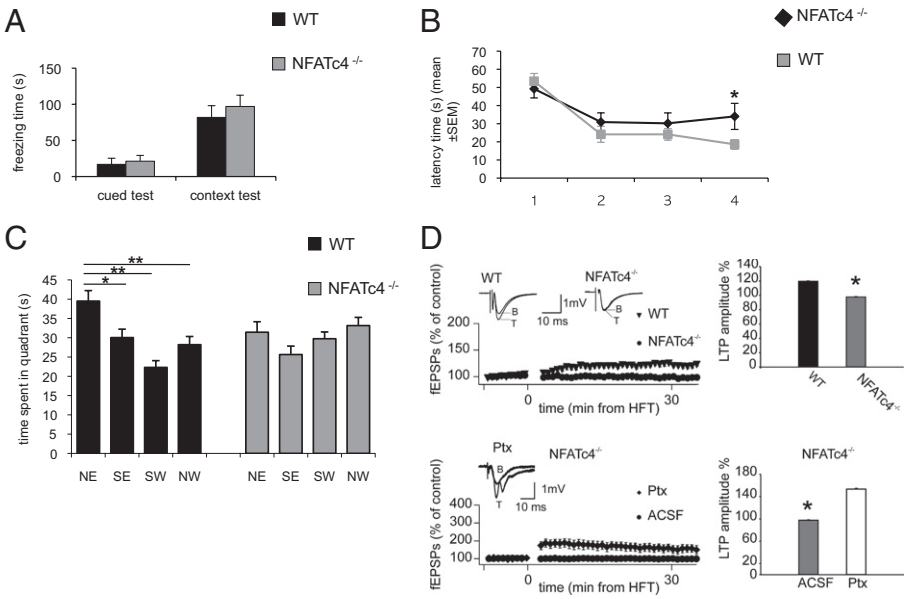

Fig. 7. NFATc4$^{-/-}$ mice show selective impairment in spatial long-term memory and LTP formation. (*A*) Contextual and cued fear conditioning. Freezing responses after training with three tone–shock pairs. Training was performed on day 1. Context test was performed on day 2. Cued (tone) test was performed on day 3. Learning was assessed by measuring freezing behavior (i.e., motionless position for ≥5 s). Data represent mean ± SEM; $n = 6$ per group. (*B*) Morris water maze 4-d training sessions for WT and NFATc4$^{-/-}$ mice. In the training phase a two-way mixed-design ANOVA also was used to check the variation between the successive trials (repeated-measures factor) and genotype (independent variable). Data represent mean ± SEM; $n = 13$ per group. *$P < 0.05$ at day 4 between WT and NFATc4$^{-/-}$ mice; Student's *t* test. (*C*) Morris water maze probe trial performed 24 h after the last training day. The probe test was analyzed separately for each genotype using one-way repeated-measures ANOVA for Bonferroni post hoc analysis (*$P < 0.05$, **$P < 0.01$). Data represent mean ± SEM; $n = 13$ per group. (*D*) DG LTP is impaired in NFATc4$^{-/-}$ mice with inhibition intact. (*Upper Left*) Summary plot illustrating the time course of changes in fEPSP slope after high-frequency stimulation (HFS) of the MPP in recordings from WT and NFATc4$^{-/-}$ mice indicates that LTP could not be detected in recordings from NFATc4$^{-/-}$ mice but was present in recordings from WT mice. (ANOVA repeated measures: WT, *$P < 0.001$, $n = 7$; NFATc4$^{-/-}$, $P = 0.853$, $n = 7$.) *Insets* illustrate typical averaged fEPSP traces obtained before (B) and after (T) LTP induction. (*Upper Right*) Summary of the changes in LTP amplitude for WT and NFATc4$^{-/-}$ mice. (WT: 120 ± 0.5%, $n = 7$; NFATc4$^{-/-}$: 98 ± 0.5%, $n = 7$; $P < 0.001$, Student's *t* test.) (*Lower Left*) Summary plot illustrating the time course of changes in fEPSP slope after high-frequency stimulation of the MPP in recordings from NFATc4$^{-/-}$ mice in control conditions (ACSF) and during picrotoxin (Ptx) application (50 μM) illustrates that LTP could be detected after inhibition was suppressed. (ANOVA repeated measures: picrotoxin, $P < 0.001$). *Inset* illustrates typical traces obtained under $GABA_A$ block (B and T as above). (*Lower Right*) Summary of the changes in LTP amplitude in control conditions and in the presence of picrotoxin. (Picrotoxin, 153 ± 1.5%; $n = 7$; ACSF, same data as in upper panels; $P < 0.001$, Student's *t* test.)

we currently cannot exclude an additional role for BDNF/calcineurin/NFATc4 signaling in surrounding cells of the adult hippocampus. Indeed, after providing evidence of NFATc4 expression in adult NSPs, we show that both expression level and transcriptional activity of NFATc4 are increased in differentiated NSPs after prosurvival BDNF administration and that NFATc4 overexpression rescues apoptosis in NFATc4$^{-/-}$ cells. As previously described, the expression of the four NFATc1-4 family members largely overlaps in the adult brain (45), but so far the functional significance of this similar expression pattern remains unclear. In our study, inhibition of both calcineurin and BDNF signaling reduces the number of adult-born hippocampal neurons in WT mice, phenocopying the NFATc4 mutants. However, the same treatments do not produce any effect in NFATc4$^{-/-}$ mice. The same is true in vitro, where the inhibition of calcineurin and BDNF signaling in differentiating WT NSPs fully blocks the prosurvival effect in WT but not in NFATc4$^{-/-}$ cells. These data suggest a major role for NFATc4, rather than the other NFAT family members, in the regulation of neural progenitor cells' survival and at the same time argue against a functional genetic redundancy among the family members in the context of adult hippocampal neurogenesis.

It should be emphasized that, even though there is mounting evidence for a critical role of calcineurin/NFAT signaling during the development of the central nervous system (22, 24, 46, 47), functional developmental abnormalities have not been found for homozygous NFATc4 mutant mice unless NFATc3 was removed also (22), thus suggesting a redundant function of NFATc4/c3 during development. The apparent redundant function of NFATc4 during development but not in the adult DG could be explained as the result of a developmental switch in NFATc4/c3 function or as a cell type-dependent difference. Interestingly, in line with this observation, recent findings suggest a cell-intrinsic responsiveness to BDNF and calcineurin signaling in different types of neurons (48). There has been speculation about what surviving newborn cells do once they start to differentiate in the DG of the adult hippocampus. Increasing evidence suggests that adult-born neurons, because of their peculiar membrane properties, might be involved in learning and memory formation, and several studies propose a role in the acquisition and storage of spatial memory (1–3, 32, 49–54). Indeed it has been demonstrated that the newborn neurons are incorporated into DG circuits supporting water maze memory (1, 55) and that spatial learning influences the survival of newborn neurons (56). These findings are consistent with our characterization of the complex phenotype of NFATc4$^{-/-}$ mice. Despite being viable, fertile, and performing normally in locomotor activity, as well as in pain sensitivity and anxiety behavior, they exhibit a selective impairment in memory formation. Interestingly, the behavioral impairment in NFATc4$^{-/-}$ mice is restricted to the formation of spatial long-term memory, because contextual long-term memory is not affected. The absence of impairment in the contextual memory tested with the fear-conditioning task as well as the impairment observed in the Morris water maze reported in our study is consistent with several but not all of the previous findings (35, 50, 51, 57). This discrepancy could be explained by differences in methods and degree of ablation of adult-born neurons used in the different studies. Furthermore the version of the Morris water maze used in the present study employs variable starting points among the trials, increasing the number of spatial representations that mice acquire during the training. Importantly, the encoding and separation of similar spatial representations (pattern separation) have been shown recently to be highly dependent on adult hippocampal neurogenesis (4, 27, 53, 57, 58). Although these results along with the electrophysiological data support a causal correlation between the reduced survival of the dentate granule neurons that we observed in NFATc4$^{-/-}$ mice and their impairment in encoding and recall of spatial long-term memory, we currently cannot exclude an additional role for NFATc4-dependent transcription in the induction of synaptic plasticity in postmitotic neurons. In summary, our data demonstrate a signaling axis between BDNF and NFATc4 in adult hippocampal neural progenitor cells and provide insight into the intrinsic regulation of hippocampal adult-born neurons survival. In conclusion, we propose that modulation of BDNF/NFATc4 signaling could represent a potential target in the therapy of

several neurological disorders where increasing the survival of endogenous or eventually transplanted progenitor cells may benefit functional recovery.

Materials and Methods

Animals. NFATc4$^{-/-}$ mice were provided and generated by the J.D.M. laboratory (59). The line was maintained on a mixed C57BL/6 and 129S7 genetic background, and littermate mice from the F2 generation, generated by interbreeding of heterozygous F1 offspring, were used. For further details see *SI Materials and Methods*.

Tissue Preparation and Immunohistochemistry. Mice were injected i.p. once or five times every 2 h with BrdU (Sigma) (150 mg/kg body weight) and were killed at 2 h or 15 or 21 d after the last injection. No mice subjected to behavioral tasks were used for the tissue studies provided here. Mice were deeply anesthetized with ketamine (120 mg/kg body weight) and xylazine (14 mg/kg body weight) and perfused intracardially with a 0.1 M PBS solution (pH 7.4) followed by 4% (vol/vol) paraformaldehyde (pH 7.4). Dissected brains were fixed further overnight at 4 °C and then were immersed for 1 d in 25% (vol/vol) sucrose/0.1 M PBS. Frozen coronal sections (30 μm) were collected throughout the entire mouse hippocampi, mounted on Superfrost slides, and stored at –20 °C until further use. For details about immunohistochemistry procedures, see *SI Materials and Methods*.

Cell Counting and Stereology. For quantification of the total number of BrdU-, Ki67-, DCX-, and calretinin-labeled cells in the DG, cells were counted using a light microscope (Zeiss).

Cell Culture of Adult Hippocampal NSPs. Adult hippocampal NSPs were obtained from WT and NFATc4$^{-/-}$ 3- to 5-mo-old male mice. For each culture, three mice were killed by cervical dislocation, and hippocampi were microdissected and pooled. For experimental details, see *SI Materials and Methods*.

Dual Luciferase Reporter Assay. Hippocampal progenitor cells derived from WT mice were seeded at a density of 1×10^5 cells into 24-well tissue-culture plates and were cotransfected with 7 μg of luciferase-based reporter constructs in which the luciferase expression is dependent on murine inositol 1,4,5-triposphate receptor 1 promoter (a gift from Armando Genazzani) and 2.7 μg of pRL –TK-*Renilla*-luciferase (Promega) according to the manufacturer's protocol (Promega). After transfection, cells were plated in culture medium for 6 h and then were switched to differentiation medium where vehicle or BDNF (100 ng/mL) was applied. After 12 h, cells were lysed and assayed for luciferase expression using a luminescence plate reader (Mithras LB940 96-well plate reader; Berthold Technologies).

RNA Extraction and Quantitative PCR. Total RNA was extracted from differentiating cells in each of the following conditions: WT vehicle-treated, WT BDNF-treated, NFATc4$^{-/-}$ vehicle-treated, and NFATc4$^{-/-}$ BDNF-treated. DNase treatment was performed using 1 μg of RNA (DNase I, amplification grade; Invitrogen) followed by cDNA synthesis (SuperScript II Reverse Transcriptase; Invitrogen), according to the manufacturer's protocol. Quantitative PCR (qPCR) was carried out using 7500 Fast Real-Time PCR System software version 2.0.4 (Applied Biosciences). Ther teaction mix was composed of SYBR Green Mix (1:2; Invitrogen), 100-nM primers (NFATc2 forward: TGGCCCGCCACATCTACCCT, reverse: TGGTAGAAGGCGTGCGGCTT; NFATc3 forward: TGGATCTCAGTATCCTTTAA, reverse: CACACGAAATACAAGTCGGA; NFATc4 forward: ACATTGAGCTACGGAAGGGTGAGA, reverse: ACTCGATGGGCACTGATGCT; BDNF forward: AAAGTCCCGGTATCCAAAGGCCAA, reverse: TAGTTCGGCATTGCGAGTTCCAGT; GAPDH forward: GCTTAAGAGACAGCCGCATCT, reverse: GCACCTTCACCATTTTGTCTACA; β-ACTINfForward: AGCCATGTACGTAGCCATCC, reverse: CTCTCAGCTGTGGTGGTGAA), and 1 μL of template (1:5 dilution of reverse transcription sample) in a total volume of 20 μL. The following cycling conditions were used: 50 °C for 20 s and 95 °C for 15 min as initial denaturation, followed by 40 cycles of 95 °C for 15 s, 60 °C for 30 s, 72 °C for 1 min. Melting curve analysis was applied afterward (95 °C for 15 s, 60 °C for 1 min, 95 °C for 30 s, 60 °C for 15 s). Samples were run in triplicate, normalized to GAPDH expression levels by applying the ΔΔCT analysis method.

Semiquantitative RT-PCR. Semiquantitative RT-PCR for *NFATc4* was performed using a thermal cycler (Applied Biosystems). The reaction mix contained TaqMan-PCR Mix (1:2; Qiagen), 400-nM primers, and 1 μL of cDNA for NFATc4 or 0.2 μL for *GAPDH* in a total volume of 25 μL. The PCR program was set to a initial denaturation at 94 °C for 5 min, followed by 45 cycles (35 cycles for *GAPDH*) of 94 °C for 30 s, 60 °C for 45 s, 72 °C for 45 s, and a final extension step at 72 °C for 5 min. PCR products were run on a 2% (vol/vol) agarose gel.

Western Blot Analysis. Protein extracts (25 μg) were prepared from E13 embryos and hippocampi of 2.5-mo-old WT and NFATc4$^{-/-}$ mice and were loaded onto 10% (vol/vol) SDS polyacrylamide gels. A nitrocellulose membrane was incubated overnight at 4 °C with primary rabbit polyclonal antibody anti-TrkB (1:1,000; Upstate) and rabbit monoclonal anti-NFATc4 (Cell Signaling). For detection of protein loading, the gel was stripped and reprobed with mouse monoclonal anti–β-actin (1:10,000; Sigma) and anti–β III-tubulin. Detection was performed by HRP-chemiluminescence (Thermo Fisher Scientific).

CsA in Vivo Treatment. CsA (40 mg/kg) (Sandimmun; Novartis) or vehicle (0.9% saline solution) was injected i.p. each day for 21 d in WT and NFATc4$^{-/-}$ mice. Mice were killed on the day of the last injection. The general health, behavior, and weight of the CsA-treated mice were normal compared with mice injected with vehicle.

Osmotic Minipump Implantation. Recombinant human TrkB-Fc chimera (100 μg) and recombinant human IgG1-Fc region (33.3 μg) (Sino Biological Inc) were infused intraparenchymally (0.5 μL/h) into the right DG of WT and NFATc4$^{-/-}$ mice for 15 d, using osmotic minipumps (Alzet #2002; Alza Corp.). Lyophilized recombinant human TrkB-Fc chimera (0.5 μg/μL) and its control peptide recombinant human IgG1-Fc (0.16 μg/μL) were reconstituted in sterile 1× PBS (Gibco). Male 2.5-mo-old mice (~30 g) were anesthetized (90 mg/kg ketamine and 10 mg/kg zylazine) and implanted with 30-gauge stainless cannulas (Alzet brain infusion kit 3; Alza Corp.) into the right DG (stereotaxic coordinates: –2.0 mm anteroposterior; +1.5 mm lateral from bregma; –2.0 mm dorsoventral) with a stereotaxic frame. Correct placement of cannulas was confirmed when animals were killed. The solutions were loaded into osmotic minipumps that then were connected to intraparenchymal cannulas by polyethylene tubing and placed s.c. Before implantation, the osmotic minipumps were primed in sterile 1× PBS (Gibco) for 48 h at 37 °C to avoid injection of air bubbles. After 15 d, mice were killed, and the brains were prepared for cryosectioning.

Behavioral Tasks. All mice used for the behavioral experiments were handled in the experimental room for 3 min on each of 2 d to minimize nonspecific emotional reactivity to the experimenter and to the room (60). The following behavioral tasks were performed: contextual and cued fear conditioning, Morris water maze, elevated plus maze, automated catwalk, and plantar heat test. For experimental details, see *SI Materials and Methods*.

Statistical Analysis. For in vitro, in vivo, and ex vivo experiments, data are shown as mean ± SEM. To determine the significance between groups, pairwise comparison was performed with the unpaired two-tailed Student's *t* test. In the Morris water maze training, latencies were analyzed using two-way mixed-design ANOVA (with genotype as independent factor and training days as repeated-measure factor). The probe test was analyzed separately for each genotype using one-way repeated-measures ANOVA. Bonferroni post hoc analysis was carried out where ANOVA data outputs were significant.

Electrophysiology. Male 2- to 4-mo-old mice were anesthetized with isoflurane and decapitated, and the brains were removed quickly. Horizontal slices (300 μm thick) containing the entorhinal cortex and the hippocampus were cut using a Leica VT1000S vibratome and were incubated for 1 h at RT in aerated (95% O2, 5% CO_2) artificial cerebrospinal fluid (ACSF) containing (in mM) NaCl 125.5, KCl 2.5, NaH_2PO_4 1.3, MgCl2 1.5, NaHCO3 26, glucose 20, CaCl2 2.5 at a pH of 7.4. Slices were transferred individually to a submerged recording chamber where they were perfused continuously with carbogenated ACSF. In a parallel set of experiments, 50 μM picrotoxin (Tocris Bioscience) was added to the ACSF bath to block $GABA_A$ receptor-mediated inhibition.

Bipolar tungsten electrodes and glass micropipettes filled with ACSF, located in the middle third of the molecular layer, were used to stimulate the MPP and record the fEPSP, respectively. Responses were evoked using short pulses (200 μs). A paired-pulse stimulus at 100-ms intervals was applied to confirm that the pathway activated was the MPP by observing paired-pulse depression. Recordings were obtained using an Axoclamp 2B amplifier (Axon Instruments). Signals were filtered at 3 kHz and then digitized. Individual synaptic responses were elicited at 20-s intervals. After a stable baseline of 10 min, LTP was induced by applying four bursts of high-frequency stimulation at 100 Hz for 1 s with a 20-s intertrain interval. Responses

were recorded for at least 35 min of LTP induction. Analysis was done using programmable Spike 2 software (Cambridge Electronic Design). IgorPro (Wavemetrics Inc.) and SigmaStat were used for statistical analysis (for details see the legend of Fig. 7*D*). The presence and amplitude of LTP were investigated by analyzing the initial slope of fEPSPs recorded over 5 min after 30 min of LTP induction and comparing those slopes with the slope of baseline recordings.

ACKNOWLEDGMENTS. We thank Armando Genazzani for providing the NFAT luciferase construct; Andreas Peter, Ricco Linder, Anja Wuttke, Paola Crociara, and Frank Baumann for technical help; and Oliver Raineteau and Gianluca Fulgenzi for helpful advice. This work was supported by funds granted by the Hertie Foundation; the Center for Integrative Neuroscience, Tübingen, Germany; the Fortune Program of the University of Tübingen; and the Deutsche Forschungsgemeinschaft (all to S.D.G.).

1. Kee N, Teixeira CM, Wang AH, Frankland PW (2007) Preferential incorporation of adult-generated granule cells into spatial memory networks in the dentate gyrus. *Nat Neurosci* 10:355–362.
2. Dupret D, et al. (2007) Spatial learning depends on both the addition and removal of new hippocampal neurons. *PLoS Biol* 5:e214.
3. Tronel S, et al. (2010) Spatial learning sculpts the dendritic arbor of adult-born hippocampal neurons. *Proc Natl Acad Sci USA* 107:7963–7968.
4. Sahay A, et al. (2011) Increasing adult hippocampal neurogenesis is sufficient to improve pattern separation. *Nature* 472:466–470.
5. Lee J, Duan W, Mattson MP (2002) Evidence that brain-derived neurotrophic factor is required for basal neurogenesis and mediates, in part, the enhancement of neurogenesis by dietary restriction in the hippocampus of adult mice. *J Neurochem* 82:1367–1375.
6. Barnabé-Heider F, Miller FD (2003) Endogenously produced neurotrophins regulate survival and differentiation of cortical progenitors via distinct signaling pathways. *J Neurosci* 23:5149–5160.
7. Sairanen M, Lucas G, Ernfors P, Castrén M, Castrén E (2005) Brain-derived neurotrophic factor and antidepressant drugs have different but coordinated effects on neuronal turnover, proliferation, and survival in the adult dentate gyrus. *J Neurosci* 25:1089–1094.
8. Bergami M, et al. (2008) Deletion of TrkB in adult progenitors alters newborn neuron integration into hippocampal circuits and increases anxiety-like behavior. *Proc Natl Acad Sci USA* 105:15570–15575.
9. Ge S, et al. (2006) GABA regulates synaptic integration of newly generated neurons in the adult brain. *Nature* 439:589–593.
10. Tashiro A, Sandler VM, Toni N, Zhao C, Gage FH (2006) NMDA-receptor-mediated, cell-specific integration of new neurons in adult dentate gyrus. *Nature* 442:929–933.
11. Zieg J, Greer PL, Greenberg ME (2008) SnapShot: Ca(2+)-dependent transcription in neurons. *Cell* 134(6):1080–1080.e2.
12. Clipstone NA, Crabtree GR (1992) Identification of calcineurin as a key signalling enzyme in T-lymphocyte activation. *Nature* 357:695–697.
13. Crabtree GR, Schreiber SL (2009) SnapShot: Ca2+-calcineurin-NFAT signaling. *Cell* 138 (1):210–210.e1.
14. Nguyen T, Di Giovanni S (2008) NFAT signaling in neural development and axon growth. *Int J Dev Neurosci* 26:141–145.
15. Hwang IK, et al. (2010) Cyclosporine A reduces dendritic outgrowth of neuroblasts in the subgranular zone of the dentate gyrus in C57BL/6 mice. *Neurochem Res* 35: 465–472.
16. Bradley KC, Groth RD, Mermelstein PG (2005) Immunolocalization of NFATc4 in the adult mouse brain. *J Neurosci Res* 82:762–770.
17. Graef IA, et al. (1999) L-type calcium channels and GSK-3 regulate the activity of NF-ATc4 in hippocampal neurons. *Nature* 401:703–708.
18. Vashishta A, et al. (2009) Nuclear factor of activated T-cells isoform c4 (NFATc4/ NFAT3) as a mediator of antiapoptotic transcription in NMDA receptor-stimulated cortical neurons. *J Neurosci* 29:15331–15340.
19. Brown JP, et al. (2003) Transient expression of doublecortin during adult neurogenesis. *J Comp Neurol* 467:1–10.
20. Bonfanti L, Theodosis DT (1994) Expression of polysialylated neural cell adhesion molecule by proliferating cells in the subependymal layer of the adult rat, in its rostral extension and in the olfactory bulb. *Neuroscience* 62:291–305.
21. Brandt MD, et al. (2003) Transient calretinin expression defines early postmitotic step of neuronal differentiation in adult hippocampal neurogenesis of mice. *Mol Cell Neurosci* 24:603–613.
22. Graef IA, Chen F, Chen L, Kuo A, Crabtree GR (2001) Signals transduced by Ca(2+)/ calcineurin and NFATc3/c4 pattern the developing vasculature. *Cell* 105:863–875.
23. Hodge RD, et al. (2008) Intermediate progenitors in adult hippocampal neurogenesis: Tbr2 expression and coordinate regulation of neuronal output. *J Neurosci* 28: 3707–3717.
24. Graef IA, et al. (2003) Neurotrophins and netrins require calcineurin/NFAT signaling to stimulate outgrowth of embryonic axons. *Cell* 113:657–670.
25. Groth RD, Mermelstein PG (2003) Brain-derived neurotrophic factor activation of NFAT (nuclear factor of activated T-cells)-dependent transcription: A role for the transcription factor NFATc4 in neurotrophin-mediated gene expression. *J Neurosci* 23: 8125–8134.
26. Xu B, et al. (2000) The role of brain-derived neurotrophic factor receptors in the mature hippocampus: mModulation of long-term potentiation through a presynaptic mechanism involving TrkB. *J Neurosci* 20:6888–6897.
27. Deng W, Aimone JB, Gage FH; (2010) New neurons and new memories: How does adult hippocampal neurogenesis affect learning and memory? *Nat Rev Neurosci* 11: 339–350.
28. Gentile CG, Jarrell TW, Teich A, McCabe PM, Schneiderman N (1986) The role of amygdaloid central nucleus in the retention of differential pavlovian conditioning of bradycardia in rabbits. *Behav Brain Res* 20:263–273.
29. Weeber EJ, et al. (2000) A role for the beta isoform of protein kinase C in fear conditioning. *J Neurosci* 20:5906–5914.
30. Phillips RG, LeDoux JE (1992) Differential contribution of amygdala and hippocampus to cued and contextual fear conditioning. *Behav Neurosci* 106:274–285.
31. Kim JJ, Fanselow MS (1992) Modality-specific retrograde amnesia of fear. *Science* 256: 675–677.
32. Snyder JS, Hong NS, McDonald RJ, Wojtowicz JM (2005) A role for adult neurogenesis in spatial long-term memory. *Neuroscience* 130:843–852.
33. Morris R (1984) Developments of a water-maze procedure for studying spatial learning in the rat. *J Neurosci Methods* 11:47–60.
34. Pellow S, Chopin P, File SE, Briley M (1985) Validation of open:closed arm entries in an elevated plus-maze as a measure of anxiety in the rat. *J Neurosci Methods* 14: 149–167.
35. Saxe MD, et al. (2006) Ablation of hippocampal neurogenesis impairs contextual fear conditioning and synaptic plasticity in the dentate gyrus. *Proc Natl Acad Sci USA* 103: 17501–17506.
36. Snyder JS, Kee N, Wojtowicz JM (2001) Effects of adult neurogenesis on synaptic plasticity in the rat dentate gyrus. *J Neurophysiol* 85:2423–2431.
37. Massa F, et al. (2011) Conditional reduction of adult neurogenesis impairs bidirectional hippocampal synaptic plasticity. *Proc Natl Acad Sci USA* 108:6644–6649.
38. Singer BH, et al. (2011) Compensatory network changes in the dentate gyrus restore long-term potentiation following ablation of neurogenesis in young-adult mice. *Proc Natl Acad Sci USA* 108:5437–5442.
39. Schmidt-Hieber C, Jonas P, Bischofberger J (2004) Enhanced synaptic plasticity in newly generated granule cells of the adult hippocampus. *Nature* 429:184–187.
40. Horsley V, Pavlath GK (2002) NFAT: uUbiquitous regulator of cell differentiation and adaptation. *J Cell Biol* 156:771–774.
41. Groth RD, Mermelstein PG (2008) NFAT-dependent gene expression in the nervous system: A critical mediator of neurotrophin-induced plasticity. *Transcriptional Regulation by Neuronal Activity*, ed Dudek SM (Springer, NewYork), 1st Ed, pp 187–207.
42. Choi SH, Li Y, Parada LF, Sisodia SS (2009) Regulation of hippocampal progenitor cell survival, proliferation and dendritic development by BDNF. *Mol Neurodegener* 4:52.
43. Thoenen H (1995) Neurotrophins and neuronal plasticity. *Science* 270:593–598.
44. Butz M, Lehmann K, Dammasch IE, Teuchert-Noodt G (2006) A theoretical network model to analyse neurogenesis and synaptogenesis in the dentate gyrus. *Neural Netw* 19:1490–1505.
45. Vihma H, Pruunsild P, Timmusk T (2008) Alternative splicing and expression of human and mouse NFAT genes. *Genomics* 92:279–291.
46. Kao SC, et al. (2009) Calcineurin/NFAT signaling is required for neuregulin-regulated Schwann cell differentiation. *Science* 323:651–654.
47. Li X, et al. (2011) Calcineurin-NFAT signaling critically regulates early lineage specification in mouse embryonic stem cells and embryos. *Cell Stem Cell* 8:46–58.
48. Rauskolb S, et al. (2010) Global deprivation of brain-derived neurotrophic factor in the CNS reveals an area-specific requirement for dendritic growth. *J Neurosci* 30: 1739–1749.
49. Kee N, Teixeira CM, Wang AH, Frankland PW (2007) Imaging activation of adult-generated granule cells in spatial memory. *Nat Protoc* 2:3033–3044.
50. Kempermann G, Gage FH (2002) Genetic determinants of adult hippocampal neurogenesis correlate with acquisition, but not probe trial performance, in the water maze task. *Eur J Neurosci* 16:129–136.
51. Zhang CL, Zou Y, He W, Gage FH, Evans RM (2008) A role for adult TLX-positive neural stem cells in learning and behaviour. *Nature* 451:1004–1007.
52. Jessberger S, et al. (2009) Dentate gyrus-specific knockdown of adult neurogenesis impairs spatial and object recognition memory in adult rats. *Learn Mem* 16:147–154.
53. Clelland CD, et al. (2009) A functional role for adult hippocampal neurogenesis in spatial pattern separation. *Science* 325:210–213.
54. Garthe A, Behr J, Kempermann G (2009) Adult-generated hippocampal neurons allow the flexible use of spatially precise learning strategies. *PLoS ONE* 4:e5464.
55. Stone SS, et al. (2011) Functional convergence of developmentally and adult-generated granule cells in dentate gyrus circuits supporting hippocampus-dependent memory. *Hippocampus* 12:1348–1362.
56. Döbrössy MD, et al. (2003) Differential effects of learning on neurogenesis: Learning increases or decreases the number of newly born cells depending on their birth date. *Mol Psychiatry* 8:974–982.
57. Dupret D, et al. (2008) Spatial relational memory requires hippocampal adult neurogenesis. *PLoS One* 3(4):e1959.
58. Aimone JB, Wiles J, Gage FH (2006) Potential role for adult neurogenesis in the encoding of time in new memories. *Nat Neurosci* 9:723–727.
59. Wilkins BJ, et al. (2002) Targeted disruption of NFATc3, but not NFATc4, reveals an intrinsic defect in calcineurin-mediated cardiac hypertrophic growth. *Mol Cell Biol* 22: 7603–7613.
60. Restivo L, Tafi E, Ammassari-Teule M, Marie H (2009) Viral-mediated expression of a constitutively active form of CREB in hippocampal neurons increases memory. *Hippocampus* 19:228–234.